

Regulation of membrane scission in yeast endocytosis

Deepikaa Menon¹ and Marko Kaksonen^{1*}

*For correspondence:

Marko.Kaksonen@unige.ch

¹Department of Biochemistry, University of Geneva, Geneva, Switzerland

Abstract

Introduction

In Clathrin-mediated endocytosis, a flat plasma membrane is pulled into a tubular invagination that eventually forms a vesicle. Forces that drive the transition from invagination to spherical vesicle in mammalian cells are provided by constriction of the GTPase Dynamin. Dynamin is now known to act in concert with the crescent-shaped N-BAR proteins Endophilin and Amphiphysin (ref. Dynamin papers). Proline-rich motifs on the Dynamin. In yeast cells, what causes membrane scission is unclear, although the yeast N-BAR protein complex Rvs has been identified as an important component of the scission module. In yeast, the Amphiphysin and Endophilin homologue Rvs is a heterodimeric complex composed of Rvs161 and Rvs167 (Friesen et al., 2006). Deletion of Rvs reduces scission efficiency by nearly 30% and reduces the invagination lengths at which scission occurs (ref Marko, wanda). Apart from a canonical N-BAR domain which forms a crescent-shaped structure, Rvs167 has a Glycine-Proline-Alanine rich (GPA) region and a C-terminal SH3 domain. Rvs161 and Rvs167 N-BAR domains are 42% similar, and 21% identical, but are not interchangeable (Sivadon, Crouzet and Aigle, 1997). The GPA region is thought to act as a linker with no known other function, while loss of the SH3 domain affects budding pattern and actin morphology. Most Rvs deletion phenotypes can however, be rescued by expression of the BAR domain alone (Sivadon, Crouzet and Aigle, 1997), suggesting that the BAR domains are the main functional unit of the Rvs complex. Homology modelling has shown that the BAR domain of Rvs167 is similar to Amphiphysin and Endophilin (Youn et al., 2010), and is therefore likely to function similarly to the mammalian homologues. In keeping with this theory, Rvs has been shown to tubulate liposomes in vitro (Youn et al., 2010). The Rvs complex arrives at endocytic sites in the last stage of the endocytosis, and disassembles rapidly at the time of membrane scission (Picco et al., 2015), consistent with a role in membrane scission. While it is known to be involved in the last stages of endocytosis, a mechanistic understanding of the influence of Rvs on scission however, remains incomplete. u89

We used quantitative live-cell imaging and genetic manipulation in *S.cereviciae* to investigate the influence of Rvs and several Rvs interacting proteins that have been suggested to have a role in scission. We found that arrival of Rvs to endocytic sites is timed by interaction of its BAR domain with a specific membrane curvature. The Rvs167 SH3 domain affects localization efficiency of the Rvs complex and also influences invagination dynamics. This indicates that both BAR and SH3 domains are important for the role of Rvs as a regulator of scission. We tested current models of membrane scission, and find that deleting yeast synaptojanins or dynamin does not change scission dynamics. Interfacial forces at lipid boundaries are therefore unlikely to be sufficient for scission, and forces exerted by dynamin are not required. Furthermore, invagination length is insensitive to overexpression of Rvs, suggesting that the recently proposed mechanism of BAR-induced protein friction on the membrane is not likely to drive scission. We propose that recruitment of Rvs BAR

43 domains prevents scission and allows invaginations to grow by stabilizing them. We also propose
 44 that vesicle formation is dependent on forces exerted by a different module of the endocytic
 45 pathway, the actin network. Preventing premature membrane scission via BAR interaction could
 46 allow invaginations to grow to a particular length and accumulate enough forces within the actin
 47 network to reliably cut the membrane.

48 Results

49 Removal of Rvs167, not Vps1, results in reduced coat movement

50 The yeast Dynamin-like protein Vps1 does not contain the canonical Proline Rich Domain, which
 51 in mammalian cells is required for recruitment to endocytic sites (ref). It is however, reportedly
 52 recruited to and interacts with endocytic proteins (refAyscough, Yu, 2004; Nannapaneni et al., 2010;
 53 Goud Gadila et al., 2017). Vps1 tagged both N- and C-terminally with GFP constructs failed to
 54 co-localize with endocytic protein Abp1 in our hands (Fig.1 supplement).

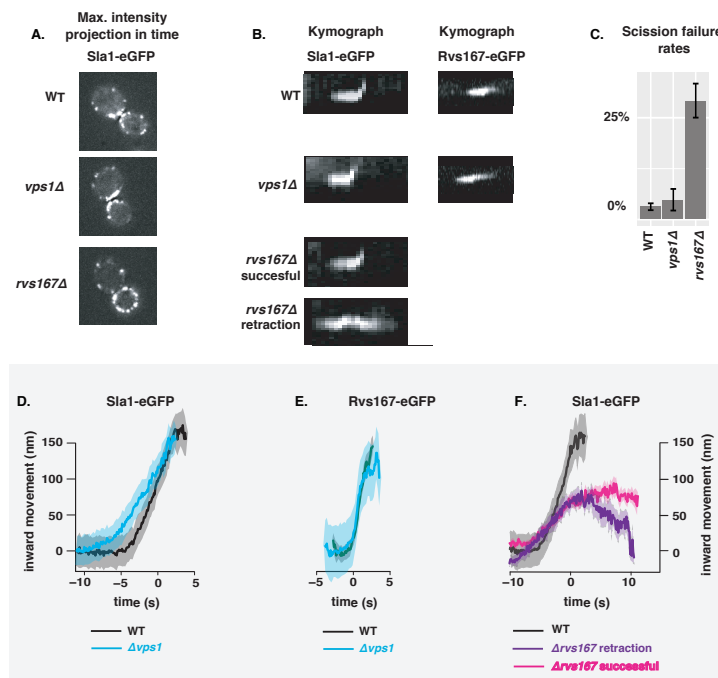


Figure 1. A: Maximum projection in time of WT, *vps1* Δ , and *rvs167* Δ cells expressing Sla1-eGFP. Scale bar= 2μm. B: Representative kymographs of Sla1-eGFP and Rvs167-eGFP patches in these cells. Scale bar x axis= (s), y axis= (nm). C: Histogram of retraction rates in WT, *vps1* Δ , and *rvs167* Δ cells, determined from tracking Sla1-eGFP in these cells. Error bars are standard deviation from two data sets, p<0.001 = *. D: Averaged centroid positions of Sla1-eGFP (D, F) in WT and *vps1* Δ cells. E: Averaged Rvs167-eGFP position in the same strains. F: Averaged Sla1-eGFP position in WT and successful and retracted Sla1-eGFP positions in *rvs167* Δ cells. All averaged positions are aligned in time to begin inward movement at the same time=0(seconds), and aligned in space to a starting position = 0 (nm). Note that in E, averaged Rvs167-eGFP inward movement is concomitant with the maxima of its fluorescent intensity (Fig1.supplement3)

55 To test whether absence of Vps1 influences scission, endocytic dynamics are observed in cells
 56 lacking Vps1 and compared against wild-type (WT) cells (Fig.1A-F). Vps1 deletion is confirmed by
 57 sequencing the open reading frame, and these cells show the growth phenotype at 37°C (Fig.1,
 58 supplement2) recorded in other work (ref. ayscough). Rates of retraction of the membrane in *vps1* Δ
 59 and WT cells is quantified by tracking the endocytic coat protein Sla1 tagged at the C-terminus with
 60 eGFP (Fig.1C). Upon actin polymerization, the endocytic coat is pulled along with the membrane as it
 61 invaginates (ref.Skrzuny?), and thus Sla1 acts as a proxy for the behaviour of the plasma membrane.
 62 Membrane retraction, that is, inward movement and subsequent retraction of the invaginated

63 membrane back towards the cell wall is a scission-specific phenotype (ref. Marko). Retraction rates
64 do not increase in *vps1Δ* cells compared to the WT (Fig.1C).

65
66

67 In order to study the total inward movement of the endocytic coat, and therefore the depth of
68 the invagination, the centroid trajectory of 50 Sla1-eGFP patches (ref. Picco, eLife 2015) in *vps1Δ*
69 and WT cells is tracked and compared (Fig.1D). In brief, yeast cells expressing fluorescently-tagged
70 endocytic proteins are imaged at the equatorial plane. Since membrane invagination progresses
71 perpendicularly to the plane of the plasma membrane, proteins that move into the cytoplasm
72 during invagination do so in the imaging plane. Centroids of 40-50 Sla1 patches- each patch being
73 an endocytic site- are tracked in time and averaged. This provides an average centroid that can be
74 followed with high spatial and temporal resolution. For more detail refer to Picco et. al, eLIFE 2015.
75 Averaged centroid movement of Sla1-eGFP in WT cells is linear to about 140nm. Sla1 movement in
76 *vps1Δ* cells has the same magnitude of movement (Fig.1D). In spite of slight differences in the rates
77 of movement, the total inward movement- and so the depth of endocytic invagination- does not
78 change.

79
80

81 Centroid tracking has shown that the number of molecules of Rvs167 peaks at the time of
82 scission, and is followed by a rapid loss of fluorescent intensity, simultaneous with a sharp jump
83 of the centroid into the cytoplasm (ref.Andrea). This jump, also seen in Rvs167-GFP kymographs
84 (Fig.1B), is interpreted as loss of protein on the membrane tube, causing an apparent spatial jump
85 to the protein localized at the base of the newly formed vesicle. Kymographs of Rvs167-GFP (Fig.1B),
86 as well as Rvs167 centroid tracking (Fig.1E) in Vps1 deleted cells show the same jump.

87
88

89 Since removal of the Rvs complex is known to increase the retraction rate at endocytic sites,
90 involvement of the Rvs proteins in the scission process was investigated further. Rvs161 and Rvs167
91 form dimers (ref.Dominik), so deletion of Rvs167 effectively removes both proteins from endocytic
92 sites. We quantified the effect of deletion of Rvs167 on membrane invagination (Fig.1A-C). 27% of
93 Sla1 patches that begin to form invaginations move inward and then retract in *rvs167Δ* cells (Fig.1C),
94 consistent with retraction rates measured in other experiments (Kaksonen, Toret and Drubin, 2005),
95 and suggesting failed scission in these 27% of endocytic events. Coat movement of the retractions
96 and of successful endocytic events were quantified (Fig.1F) as described in Picco et. al, 2015. Sla1
97 centroid movement in both successful and retracting endocytic events in *rvs167Δ* cells and WT
98 look similar up to about 60nm (Fig.1F). In successful endocytic events, Sla1-egfp signal is then lost,
99 similar to WT cells, and Abp1 intensity drops (Fig.1supplement), indicating that scission occurs at
100 invagination lengths between 60 -80 nm. That membrane scission occurs at shorter invagination
101 lengths than in WT is corroborated by the smaller vesicles formed in *rvs167Δ* cells by Correlative
102 light and electron microscopy (CLEM) (Kukulski et al., 2012). In retraction events, the Sla1 centroid
103 moves back towards its original position. CLEM has also shown that Rvs167 localizes to endocytic
104 sites after the invaginations are about 60nm long (Kukulski et al., 2012). Sla1 movement in *rvs167Δ*
105 indicates therefore that membrane invagination is unaffected till Rvs is supposed to arrive.

106 **Synaptojanins likely influence vesicle uncoating, but not scission dynamics.**

107 There are three Synaptojanin-like proteins in budding yeast: Inp51, Inp52, and Inp53 (Fig2a). Inp51-
108 eGFP exhibits a diffuse cytoplasmic signal, and Inp53 localizes to patches within the cytoplasm-
109 cellular localization that is consistent with involvement in trans-Golgi signalling (refGolgi)- Inp53
110 was not investigated further. Inp52-eGFP localizes to cortical actin patches that are endocytic sites
111 (Fig2 supplement). Spatial and temporal alignment with Sla1 and Rvs167 shows that Inp52 protein
112 molecules arrive in the late scission stage, and localizes to the bud tip, consistent with a role in

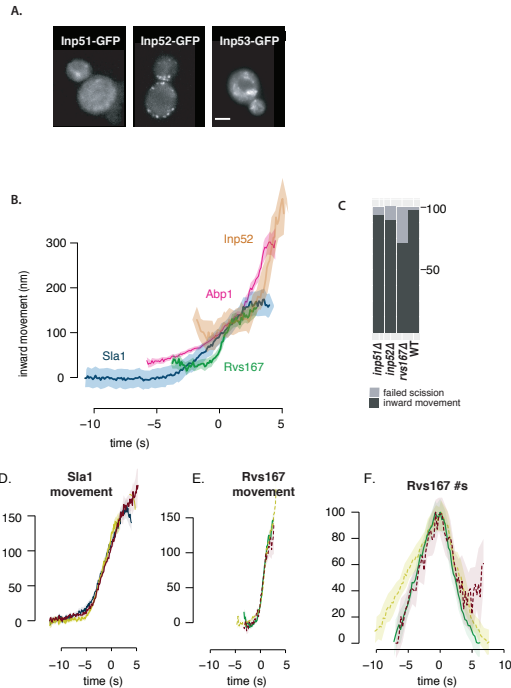


Figure 2. A half-columnwidth image using wrapfigure, to be used sparingly. Note that using a wrap figure before a sectional heading, near other floats or page boundaries is not recommended, as it may cause interesting layout issues. Use the optional argument to wrapfigure to control how many lines of text should be set half-width alongside it.

113 membrane scission (Fig.2b).

114 Inp51 and Inp52 were tested as potential candidates for scission regulators. Sla1-eGFP and
 115 Rvs167-eGFP in cells with either Inp51 or Inp52 deleted were studied. Retraction events do not
 116 significantly increase compared to the WT in either *inp51* Δ or *inp52* Δ cells (Fig2c). Magnitude and
 117 speed of coat movement in *inp51* Δ is the same as the WT (Fig2.d). In *inp52* Δ cells, coat movement
 118 also has the magnitude and speed as WT, but Sla1-eGFP signal is persistent after membrane scission
 119 (Fig.2d). Similarly, although Rvs167 inward movement looks the similar (Fig2e), disassembly has a
 120 delay, while the assembly is similar to WT (Fig2f). Assembly of Rvs167 has a delay in *inp51* Δ cells.
 121 The magnitude of the inward movement of both Sla1 and Rvs167 in cells containing either deletion
 122 are the same as in WT, while assembly and disassembly dynamics of Rvs167 is changed.

123 **Rvs BAR domains recognize membrane curvature in-vivo**

124 The interaction between Rvs167 and membrane curvature *in vivo* has not so far been tested. In
 125 order to do so, we deleted the SH3 domain of Rvs167 leaving the N-terminal BAR region (henceforth
 126 BAR-GPA) and observed the localization of full-length Rvs167 and BAR-GPA (Fig3a). The GPA region
 127 is a disordered region that has no previously reported function and was retained to ensure proper
 128 folding and function of the BAR domain. Endogenously tagged Rvs167-eGFP and BAR-GPA-eGFP
 129 colocalization with Abp1-mCherry in WT and *sla2* Δ cells are compared (Fig3b). Sla2 acts as the
 130 molecular linker between forces exerted by the actin network and the plasma membrane (ref.
 131 Skruzny). *sla2* Δ cells therefore contain a polymerizing actin network at endocytic patches, but the
 132 membrane remains flat and endocytosis fails. In these cells, the full-length Rvs167 protein co-
 133 localizes with Abp1-mCherry, indicating that it is recruited to endocytic sites (Fig3b). BAR-GPA-eGFP
 134 localization is removed, except for rare transient patches that do not co-localize with Abp1-mCherry,
 135 indicating that in the absence of membrane curvature, the BAR domains cannot localize to endocytic
 136 sites (Fig3b, *sla2* Δ).

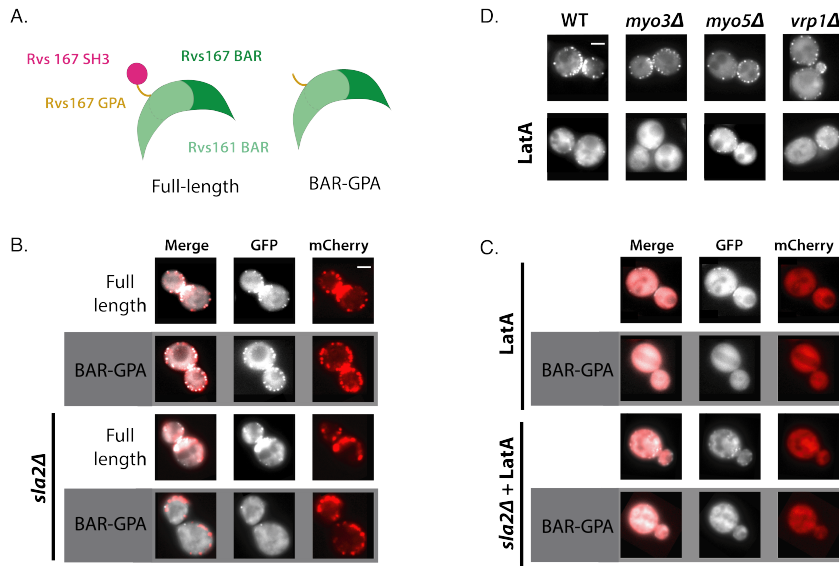


Figure 3. A half-columnwidth image using wrapfigure, to be used sparingly. Note that using a wrap figure before a sectional heading, near other floats or page boundaries is not recommended, as it may cause interesting layout issues. Use the optional argument to wrapfigure to control how many lines of text should be set half-width alongside it.

137 **SH3 domains are likely recruited by Myosin 3**

138 SH3 domains have been shown to interact with several proteins in the actin module of endocytosis.
 139 Type I myosins Myo3 and Myo5, and Vrp1 have genetic or physical interactions with Rvs167 SH3
 140 domains (Lila and Drubin, 1997; Colwill et al., 1999; Madania et al., 1999; Liu et al., 2009). We tested
 141 the interaction between these proteins and the Rvs167-SH3 region by studying the localization of
 142 full-length Rvs167 in cells with one of these proteins deleted, and treated with LatA to reproduce
 143 the situation in which BAR-curvature interaction is removed, and SH3 interaction remains. Deletion
 144 of neither Vrp1 nor Myo5 in combination with LatA treatment removes the localization of Rvs167.
 145 Deletion of Myo3 with LatA treatment removes localization of Rvs167.

146 what about the differences in myo5 and myo3 number...

147 **Loss of Rvs167 SH3 domain affects coat and actin dynamics**

148 In order to further probe the contribution of the Rvs167 SH3 domain to endocytosis, we compared
 149 dynamics of Sla1, as well as Rvs167 and BAR-GPA centroids (Fig4a). Movement of Sla1 centroid is
 150 reduced in BAR-GPA cells (Fig4a). Both full length Rvs167 and BAR-GPA however, arrive at endocytic
 151 coats when Sla1 centroid is about 30nm away from the initial position (Fig1a, red line to the y axis).
 152 Tubular invaginations are formed in BAR cells, and qualitatively resemble that in WT cells, as seen by
 153 CLEM (Fig.4 supplement). The inward jump of BAR-GPA is less than that of full-length Rvs167 (Fig.4b).
 154 Recruitment of BAR is reduced to half that of Rvs167 (Fig4c), although cytoplasmic concentration of
 155 Rvs167 and BAR are not different (Fig4 supplement). We also quantified the number of Abp1 and
 156 Rvs molecules recruited to endocytic sites (Fig4b). Abp1 disassembly is slowed down in BAR-GPA
 157 cells compared to WT (Fig4b), and recruitment is reduced to 50% of WT recruitment (Fig.4c), likely
 158 indication disruption of actin network assembly.

159 **N-helix and GPA domains do not contribute to recruitment of Rvs or membrane 160 movement**

161 Etiam euismod. Fusce facilisis lacinia dui. Suspendisse potenti. In mi erat, cursus id, nonummy
 162 sed, ullamcorper eget, sapien. Praesent pretium, magna in eleifend egestas, pede pede pretium
 163 lorem, quis consectetur tortor sapien facilisis magna. Mauris quis magna varius nulla scelerisque

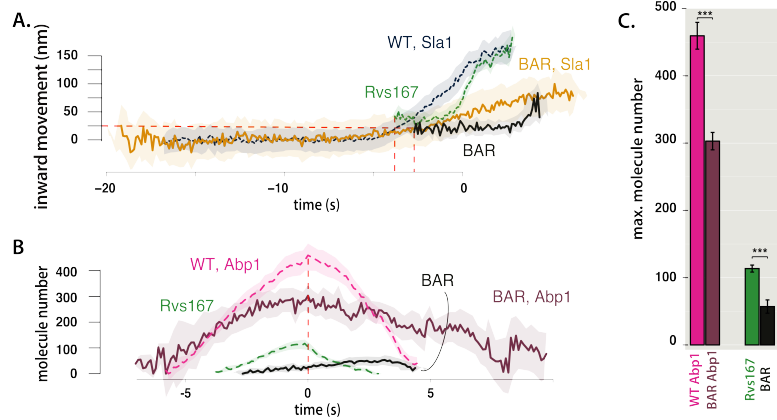


Figure 4. A half-columnwidth image using wrapfigure, to be used sparingly. Note that using a wrapfigure before a sectional heading, near other floats or page boundaries is not recommended, as it may cause interesting layout issues. Use the optional argument to wrapfigure to control how many lines of text should be set half-width alongside it.

164 imperdiet. Aliquam non quam. Aliquam porttitor quam a lacus. Praesent vel arcu ut tortor cursus
 165 volutpat. In vitae pede quis diam bibendum placerat. Fusce elementum convallis neque. Sed dolor
 166 orci, scelerisque ac, dapibus nec, ultricies ut, mi. Duis nec dui quis leo sagittis commodo.

167 **Reduced BAR domain recruitment corresponds to reduced membrane movement**

168 Decreased Sla1 movement in BAR-GPA cells (Fig4a) can be explained by loss of some interaction
 169 mediated by the SH3 domain, or because the BAR-GPA mutant is recruited in smaller numbers to
 170 endocytic sites. To check whether increasing the recruitment of the Rvs complex alone can rescue
 171 reduced Sla1 movement, Rvs167 and Rvs161 genes were duplicated endogenously (ref Huber) in
 172 diploid and haploid yeast cells. Diploid cells are thus generated containing either 4 copies of both
 173 Rvs genes (by gene duplication), 2 copies of each gene (WT diploid), or 1 copy (by deleting one copy
 174 of Rvs167 and Rvs161). In diploid cells (Fig5a-c), amount of Rvs167 recruited to sites increases with
 175 gene copy number (Fig5c). Adding excess Rvs to endocytic sites in the 4x case does not change
 176 the rate or total inward movement of Sla1, or of Rvs167. In the case of 1x Rvs, Sla1 movement is
 177 slightly reduced after 100nm (Fig5a). Magnitude of Rvs167 inward movement is unchanged, but the
 178 Rvs167-eGFP signal is lost immediately after the inward movement, unlike in the 4x and 2x cases. In
 179 haploid cells, increasing the number of Rvs167 and Rvs161 genes results in increased recruitment
 180 of Rvs167 to about 1.6 times the WT amount (Fig5f,h). Sla1 dynamics however, remains the same
 181 as in the WT(Fig5d). Duplicating the BAR-GPA domain alone rescues the loss of Sla1 movement
 182 in the 1x BAR-GPA, as well the inward jump of BAR-GPA itself (Fig5d,e). We measured the total
 183 number of Abp1 molecules at endocytic sites for different strains (Fig5g,h), and found that higher
 184 Abp1 numbers corresponds to larger Sla1 centroid movement. Total Abp1 numbers recruited are
 185 reduced for 1xBAR and rvs167Δ strains (Fig5g,h), suggesting a correlation between the maximum
 186 number of Abp1 recruited and total invagination length.

187 **Discussion**

188 Recruitment and function of the Rvs complex in has been explored in this work, as well as several
 189 models for how membrane scission could be effected in yeast endocytosis. We propose that
 190 Rvs is recruited to endocytic sites by interactions between the Rvs BAR domains and invaginated
 191 membrane, and that SH3 domain mediated protein-protein interactions are required for efficient
 192 recruitment of Rvs to sites. Arrival of Rvs on membrane tube scaffolds the membrane and prevents
 193 premature membrane scission. Effective scaffolding depends on recruitment of a critical number
 194 of Rvs molecules. Rvs is a relatively short-lived protein at endocytic sites. It is recruited only once

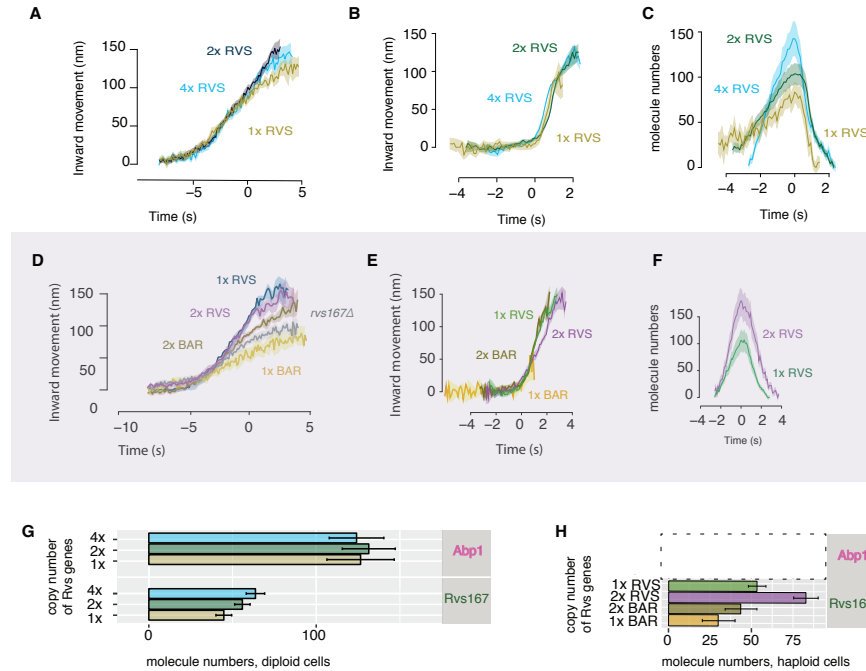


Figure 5. A half-columnwidth image using wrapfigure, to be used sparingly. Note that using a wrapfigure before a sectional heading, near other floats or page boundaries is not recommended, as it may cause interesting layout issues. Use the optional argument to wrapfigure to control how many lines of text should be set half-width alongside it.

membrane tube is formed (Kaksonen, Toret and Drubin, 2005; Kukulski et al., 2012; Picco et al., 2015). FCS measurements (Boeke et al., 2014) have shown that the cytosolic concentrations of Rvs167 and Rvs161 are high (354nM and 721nM respectively) compared to other endocytic proteins like Las17, Vrp1, Myo3, and Myo5 (80-240nM). In spite of this, relatively few numbers of Rvs are recruited to endocytic sites, suggesting that recruitment is tightly regulated. In the case of Rvs, both timing and efficiency appear crucial to its function, the question is what confers both.

201 **BAR domains sense *in vivo* membrane curvature and time recruitment of Rvs**

202 The curved structure of BAR dimers (Peter et al., 2004; Mim et al., 2012) has suggested that Rvs
 203 is recruited by its preference for some membrane shapes over others, supported by its arrival at
 204 curved membrane tubes. In the absence of membrane curvature, in *sla2Δ* cells, the BAR domain
 205 alone does not localize to cortical patches (Fig.3b,c). This demonstrates for the first time that the
 206 BAR domain does indeed sense and requires membrane curvature to localize to cortical patches.
 207 Work on BAR domains have proposed that electrostatic interactions at the concave surface and
 208 tips of the BAR domain structure mediate membrane binding (Qualmann, Koch and Kessels, 2011).
 209 Mutations in these lipid-binding surfaces would clarify the interaction with underlying lipids, and
 210 test if Rvs relies on similar interactions. BAR is able to localize to endocytic sites, and has a similar
 211 lifetime in WT cells (Fig.4b). However, time alignment with Abp1 shows that there is a delay in the
 212 recruitment of BAR-GPA compared to Abp1 arrival, compared to full-length Rvd167 (Fig4c). The
 213 delayed recruitment occurs because the invagination takes longer to reach a particular length: Sla1
 214 moves inwards at a slower rate in BAR cells, and it takes longer for the membrane in BAR-GPA cells
 215 to reach the same length as Rvs167. Rvs167 arrives in BAR cells when Sla1 has moved inwards
 216 25-30nm (dashed red lines in Fig.4a), which is also the distance Sla1 has moved when Rvs167 arrives
 217 in WT. By the time Sla1 has moved this distance, the membrane is already tubular (Kukulski et

218 al., 2012; Picco et al., 2015), consistent with Rvs arrival at invaginated tubes. This suggests Rvs
219 recruitment is timed to specific membrane invagination length- therefore to a specific membrane
220 curvature- and that this timing is provided by the BAR domain.

221 **SH3 domains allow efficient and actin independent recruitment**

222 Rvs167 in BAR cells accumulates to about half the WT number (Fig.3c), even though the same cyto-
223 plasmic concentration is measured (supplement Fig3?), indicating that the SH3 domain increases
224 the efficiency of recruitment of Rvs. In *sla2Δ* cells, full-length Rvs can assemble on the membrane
225 (Fig.3b,c). Since BAR domains alone do not localize to patches in *sla2Δ* cells, full-length localization
226 must be mediated by the SH3 domain, supporting a role for the SH3 domain in increasing
227 recruitment of Rvs by clustering protein molecules. That full-length Rvs167 is able to assemble and
228 disassemble at cortical patches in *sla2Δ* cells without the curvature- dependent interaction of the
229 BAR domain (Fig.3b,c) indicates that the SH3 domain is able to mediate both the recruitment and
230 the disassembly of Rvs at the endocytic site. In *sla2Δ* cells treated with LatA (Fig.3c), actin-based
231 membrane curvature is inhibited, and the actin patch proteins are removed from the plasma mem-
232 brane. Full-length Rvs167 in these cells still shows transient localizations at the plasma membrane.
233 In *sla2Δ* cells treated with LatA, the localization of BAR is lost. This suggests that localization of the
234 full-length Rvs167 in LatA treated cells is dependent on an SH3 domain interaction, and that this is
235 independent of both actin and membrane curvature.

236 In WT cells, the Abp1 and Rvs167 fluorescent intensities reach maxima concomitantly (Fig4b),
237 and the consequent decay of both also coincide. Coincident disassembly indicates that upon vesicle
238 scission, the actin network is immediately disassembled. Membrane scission essentially occurs
239 around the intensity peak of the two proteins. This coincident peak is lost in BAR-GPA cells: BAR-
240 GPA-eGFP in these cells peaks several seconds after Abp1 intensity starts to drop, and the decay of
241 Abp1 is prolonged, taking nearly double the time as in WT. The number of Abp1 molecules recruited
242 is decreased to about two thirds the WT number. Although it is not clear what the decoupling of
243 Abp1 and Rvs peaks means, the changes in Abp1 dynamics suggests a strong disruption of the actin
244 network dynamics. SH3 domains are known to interact with components of the actin network like
245 Abp1 and Las17 (Lila and Drubin, 1997, Madania et al., 1999), but study of other components of
246 the actin machinery will be required to understand how exactly loss of the SH3 has changed the
247 progression of endocytosis.

248 SH3 interaction with an endocytic binding partner likely help recruit Rvs to endocytic sites. Many
249 such interaction partners have been proposed. Abp1 interaction with the Rvs167 SH3 domain
250 has been shown (Lila and Drubin, 1997; Colwill et al., 1999), as has one with WASP protein Las17
251 (Madania et al., 1999; Liu et al., 2009), yeast Calmodulin Cmd1 (Myers et al., 2016), type I myosins
252 (Geli et al., 2000), and Vrp1 (Lila and Drubin, 1997). All of these suggested binding partners localize
253 to the base of the invagination (Yidi Sun, 2006; Picco et al., 2015), and do not follow the invaginating
254 membrane into the cytoplasm. The SH3 interaction partner is likely Myo3 (Fig3d), and SH3 domains
255 interact with the endocytic network at the base of the invagination. Centroid tracking however,
256 suggests that Rvs is accumulated all over the membrane tube. If Rvs was recruited to the base and
257 pulled up as the invagination grows, the centroid would move continuously upwards rather than
258 remain relatively non-motile before the jump at scission time. It is possible that the SH3 initially
259 helps cluster near the base, and as the membrane invaginations grow longer, BAR-membrane
260 interactions dominate.

261 **Accumulation of Rvs on membrane invagination**

262 When ploidy is doubled from haploid to diploid yeast cells, we could expect that double the protein
263 amount is expressed and recruited, but it does not appear so. The amount of Rvs recruited in
264 WT haploid and diploids remains about the same, and cytoplasmic signal is similar (Fig.5, Fig5
265 supplement). This invariance between accumulated protein in haploids and diploids shows that Rvs
266 recruitment is not determined by the number of alleles of Rvs. Haploid and diploid cells appear

267 to tune the amount of Rvs recruitment to get a specific amount to endocytic sites. WT diploids
268 (2xd) contain two copies each of RVS161 and RVS167 genes. Rvs duplicated diploids, which contain
269 four copies each of RVS167 and RVS161 (4xd) could be expected to express and recruit to sites
270 twice the amount of Rvs as 2xd. However, compared to 2xd, cytoplasmic signal in 4xd increases
271 by 1.6x and recruitment of Rvs167 to endocytic sites increases only by 1.4x. Doubling the gene
272 copy number increases, but does not double protein expression or recruitment in the case of
273 Rvs. Similarly, duplicating Rvs genes in haploid cells results in an increase in number of molecules
274 recruited, but not in doubling (1xh, 2xh). Although the rate of adding Rvs is different in haploids and
275 diploids, in both cases, it increases by gene copy number (yellow line in Fig.4.2). Cytoplasmic protein
276 concentration is increased when gene copy number is increased, and recruitment to endocytic
277 sites is increased by the increase in cytoplasmic concentration. These data suggest that the amount
278 of Rvs that is recruited scales with available concentration of protein. Comparing across ploidy
279 however, the rate of Rvs recruitment is lower in WT diploid compared to WT haploid (2xd vs 1xh,
280 Fig.4.1)

281 for this is not clear. 4.2 Arrangement of Rvs dimers on the membrane A homology model of
282 the Rvs BAR dimer structure based on Am-phiphysin suggests that it has the concave structure
283 typical for N-BAR domains. Rvs is a hetero- rather than homodimer unlike Am-phiphysin, and a
284 high-resolution structure will be necessary to clarify the interaction and arrangement of Rvs on
285 endocytic tubes. There are some indications from the experiments in this thesis however, regarding
286 its interaction with the membrane. 4.2.1 Rvs does not form a tight scaffold on membrane tubes
287 Observations of *in vitro* helices of BAR domains have suggested that Rvs might form a similar helical
288 scaffold. The number of Rvs molecules recruited to endocytic sites is high enough to cover the
289 surface area of the tubular invagination, so it has been proposed that an Rvs scaffold covers the
290 entire membrane tube up to the base of the future vesicle (Picco et al., 2015). In Rvs duplicated
291 diploid cells (4xd), Rvs can be recruited at a much faster rate than in the WT (2xd) (Fig.3.10B-
292 C, Fig.4.2) while disassembly dynamics is the same in both (Fig.3.10C, Fig.4.3). The exponential
293 decay of fluorescent intensity in WT haploid and diploid cells (1xh, 2xd, Fig.4.3) indicates that
294 all of the protein is suddenly disassembled from the endocytic site. When the membrane tube
295 undergoes scission, there is no more tubular curvature for the Rvs to bind to. The sharp decay is
296 therefore consistent with a BAR scaffold that breaks upon vesicle scission because there is no more
297 membrane interaction, releasing all the membrane-bound protein at once. A similar decay in the
298 4xd strain suggests that all the Rvs in this case is also bound to the membrane: if the protein was
299 not bound to the membrane, fluorescent intensity would not decay sharply. Since the membrane is
300 able to accommodate 1.4x the amount of BAR protein as the WT, it would suggest that at lower
301 protein amounts, a tight helix that covers the entire tube is not likely. Adding molecules to a tube
302 already completely covered by a scaffold would result in a change in Rvs assembly and disassembly
303 dynamics. Further, additional molecules would have to be added at the top or base of a tight
304 scaffold. At the top, the radius of curvature is decreased compared to the tube since this is the
305 rounded vesicle region. At the base, the plasma membrane is nearly flat, and the Rvs BAR domain
306 is similarly unlikely to favour interactions here. Otherwise the scaffold would have to be disrupted
307 to add new molecules, which would likely slow down recruitment rate rather than speed it up.
308 Molecules could also be added concentric to an existing scaffold. However, the concave surface of
309 Rvs is known to interact with lipids, and multiple layers of BAR domains on the membrane tube
310 would probably not show the sudden disassembly seen here. I assume that the membrane surface
311 area does not change in the 4xd compared to 2xd from the identical movement of Sla1 in both
312 cases (Fig.3.10A). It is possible that a wider tube is formed, which would increase the membrane
313 surface area for BAR binding. This would, however, require the BAR domains to interact with a lower
314 radius of curvature than in WT. This seems unlikely, and in the absence of any indication otherwise,
315 I assume that the membrane tubes in all diploid and haploid cases have the same width. 4.2.2 A
316 limit for how much Rvs can be recruited to the membrane In the case of Rvs duplication in haploids
317 (2xh), a change in disassembly dynamics is seen (Fig.3.9C, Fig.4.3). In 2xh, the maximum number

318 of molecules recruited is 178 ± 7.5 compared to the maximum of 113.505 ± 5.2 in WT (1xh). This is
319 means that nearly 1.6x the WT amount of protein is recruited to membrane tubes in the 2xh case.
320 The Rvs167 fluorescent intensity in 2xh shows a delay in disassembly. This suggests that the excess
321 protein may not be directly on the membrane, since if the protein was membrane bound, when the
322 membrane breaks, the protein must be released. The excess Rvs could either interact with the actin
323 network via the SH3 domain, or interact with other Rvs dimers. By a similar argument as in 4.2.1
324 above, I do not expect that multiple layers of BAR domains are formed, and that the excess protein
325 is recruited by the interaction of the SH3 domain. Another explanation for the delayed disassembly
326 is that at high concentrations of Rvs like in the 2xh case, a tight BAR scaffold is formed, and the
327 BAR domains interact with adjacent BAR domains. When the membrane undergoes scission, the
328 protein is no longer membrane-bound, but lateral interactions delay disassembly of the scaffold.
329 Lateral interactions between neighbouring BAR dimers have been shown in the case of Endophilin
330 (Mim et al., 2012). It is not currently clear where the Rvs molecules are added in the 2xh case:
331 superresolution microscopy could clarify whether it is added at the membrane tube. Whatever
332 the arrangement of the Rvs complex on the membrane, disassembly dynamics is changed in the
333 case of 2xh, compared to the other haploid and diploid strains. Since the number of Rvs molecules
334 is highest in this strain, this suggests that there is a limit to how much Rvs can assemble on the
335 tube without altering interaction with the endocytic protein network. 4.2.3 Conclusions for Rvs
336 localization All of these data support the idea that Rvs recruitment rate and total numbers are
337 determined by concentration of protein in the cell. The maximum number of molecules that can
338 interact with the membrane is limited by the surface area of the invagination. Although more can
339 be recruited, Rvs molecules over a certain threshold interact in a different way with endocytic sites,
340 possibly via the SH3 domain. Timing of recruitment to sites is by curvature-recognition via the BAR
341 domain, while efficiency of recruitment and interaction with the actin network is established via the
342 SH3 domain. 4.3 What causes membrane scission?

343 **Rvs acts as a membrane scaffold preventing membrane scission**

344 Invaginations in *rvs167Δ* cells undergo scission at short invagination lengths of about 80nm (Fig.3.2),
345 compared to the WT lengths of 140nm. This shows that first, enough forces are generated at
346 80nm to cause scission. Then, that Rvs167 is required at membrane tubes to prevent premature
347 scission. Prevention of scission at short invagination lengths can be explained by Rvs stabilizing
348 the membrane invagination via membrane interactions of the BAR domain (Boucrot et al., 2012;
349 Dmitrieff and Nedelec, 2015). Rvs preventing membrane scission could also be explained by the
350 SH3 domain mediating actin forces to the invagination neck: one can imagine that the SH3 domain
351 somehow decouples actin forces from the neck, and that this delays scission. Since invagination
352 lengths of *rvs167a* cells are increased towards WT by overexpression of the BAR domain alone
353 (Fig.3.12A), I propose that localization of Rvs BAR domains to the membrane tube stabilizes the
354 membrane. This allows deep invaginations to grow until actin polymerization produces enough
355 forces to overcome this stabilization and sever the membrane. Stabilization of the membrane
356 tube increases with increasing amounts of BAR domains recruited to the membrane tube (Fig.3.12).
357 The requirement for Rvs scaffolding cannot be removed by reducing turgor pressure (Fig.3.13),
358 suggesting that the function of the scaffold is not to counter turgor pressure.

359
360 Scission efficiency decreases with decreased amounts of Rvs: in diploids, lowering the amount
361 of Rvs by 20 molecules decreases scission efficiency to about 90% from 97%. This indicates that
362 a particular coverage of the membrane tube is required for effective scaffolding by BAR domains.
363 In support of this, in BAR strains, fewer numbers of Rvs are recruited, and scission efficiency is
364 similarly reduced. At low concentrations of Rvs like in the 1xd cells, it is likely that some membrane
365 tubes recruit the critical number of Rvs, in which case the invaginations grow to near WT lengths.
366 Over a certain amount of Rvs, adding more BAR domains does not increase the stability of the
367 tube: in 4xd, the same amount of actin is recruited before scission as in the 2xd and 1xd strains. If

368 enough forces are generated at 80nm, why is scission efficiency decreased in *rvs167Δ* compared
369 to WT? Forces from actin may be at a threshold when the invagination is at 80nm. There could be
370 enough force to sever the membrane, but not enough to sever reliably. The Rvs scaffold then keeps
371 the network growing to accumulate enough actin to reliably cause scission. Controlling membrane
372 tube length could also be a way for the cell to control the size of the vesicles formed, and therefore
373 the amount of cargo packed into the vesicle.

374 **What causes membrane scission?**

375 We have tested several scission models that include a major role for the Rvs complex. The seemingly
376 obvious solution to the scission problem is the action of a dynamin-like GTPase. If loss of the yeast
377 Dynamin Vps1 prevented or delayed scission, the membrane would continue to invaginate longer
378 than WT lengths, and Sla1 movements of over 140nm should be observed. Rvs centroid movement
379 would likely also be affected: a bigger jump inwards could indicate that a longer membrane has
380 been cut. That neither is seen in the behaviour of coat and scission markers indicates that even if
381 Vps1 is recruited to endocytic sites, it is not necessary for Rvs localization or function, and is not
382 necessary for scission. The Inp51, Inp52 data tests the lipid hydrolysis model, in which synaptojanins
383 hydrolyze PIP2 molecules that are not covered by BAR domains, resulting in a boundary between
384 hydrolyzed and non- hydrolyzed PIP2. This model predicts that interfacial forces generated at the
385 lipid boundary causes scission (Liu et al., 2006). Inp51 is not seen in patches at the cellular cortex,
386 but this could be because protein recruitment is below our detection threshold. Inp52 localizes to
387 the top of invaginations right before scission, consistent with a role in vesicle formation (Fig.3.7D).
388 Some predictions of the lipid hydrolysis model are inconsistent with our data, however. First, vesicle
389 scission is expected to occur at the interphase of the hydrolyzed and non-hydrolyzed lipid. Since the
390 BAR scaffold covers the membrane tube, this interphase would be at the top of the area covered by
391 Rvs. Kukulski et al., 2012 have shown that vesicles undergo scission at 1/3 the invagination length
392 from the base: that is, vesicles generated by the lipid boundary would be smaller than have been
393 measured. Second, removing forces generated by lipid hydrolysis by deleting synaptojanins should
394 increase invagination lengths, since scission would be delayed or it would fail without those forces.
395 Deletion of neither Inp51 nor Inp52 changes the invagination lengths: Sla1 movement does not
396 increase. That the position of the vesicle formed is also unchanged compared to WT is indicated by
397 the similar magnitude of the jump into the cytoplasm of the Rvs centroid. There are some changes
398 in the synaptojanin deletion strains (Fig.3.8). In *inp51Δ* cells, Rvs assembly is slightly slower than
399 that in WT. Therefore, Inp51 could play a role in Rvs recruitment. In the *inp52Δ* strain, about 12% of
400 Sla1-GFP tracks retract, indicated that scission fails in those cases. Although this is low compared to
401 the failed scission rate of *rvs167Δ* cells (close to 30%), this data could suggest a moderate influence
402 of Inp52 on scission. Rvs centroid persists after scission for about a second longer in *inp52Δ* cells
403 than in WT, indicating that disassembly of Rvs on the base of the newly formed vesicle is delayed.
404 Inp52 is likely involved in vesicle un- coating. Deletion of synaptojanin-like Inp52 does not affect the
405 movement of the invagination. In spite of this, Sla1 patches persist for longer after scission in the
406 *inp52Δ* than in WT cells, as does Rvs167, indicated by the arrows in Fig.3.8A,D. Persistence of both
407 suggests that rather than the scission timepoint, post-scission disassembly of proteins from the
408 vesicle is inhibited in *inp52Δ* cells. Inp52 then plays a role in recycling endocytic proteins from the
409 vesicle to the plasma membrane. The slower assembly of Rvs in *inp51Δ* and the increase in coat
410 retraction rates of *inp52Δ* could indicate that there is a slight effect on Rvs recruitment, and that
411 lipid hydrolysis could play a small role in scission.

412
413 Protein-friction mediated membrane scission proposes that BAR domains induce a frictional force
414 on the membrane, causing scission. In Rvs duplicated haploid cells (2xh), adding up to 1.6x the
415 WT (1xh) amount of Rvs to membrane tubes does not affect the length at which the membrane
416 undergoes scission (Fig.3.9). If more BAR domains were added to the membrane tube, frictional
417 force generated as the membrane is pulled under it should increase, and the membrane should

418 rupture faster. That is, membrane scission occurs as soon as WT forces are generated on the tube.
419 Since BAR domains are added at a faster rate in the 2xh cells, these forces would be reached at
420 shorter invagination lengths. In 2xh cells, WT amount of Rvs is recruited at about 1.8 seconds before
421 maximum fluorescent intensity, but scission does not occur at this time. Instead, Rvs continues
422 to accumulate, and the invagination continues to grow. In diploid strains, adding 1.4x the WT
423 amount of Rvs in the 4x Rvs case also does not change length of membrane that undergoes scission.
424 Therefore, protein friction due to Rvs does not appear to contribute significantly to membrane
425 scission in yeast endocytosis.

426 Maximum amount of Abp1 measured in all the diploid strains is about 220 molecules (Fig.3.11).
427 In this case, only one allele of Abp1 is fluorescently tagged, so half the amount of Abp1 recruited
428 is measured. The maximum amount of Abp1 recruited is then double that measured, which is
429 about 440 ± 20 molecules (assuming equal expression and recruitment of tagged and untagged
430 Abp1). In WT haploid cells, the maximum number of Abp1 measured is 460 ± 20 molecules. That the
431 same number of molecules of Abp1 is recruited in all cases before scission indicates that scission
432 timing depends on the amount of Abp1, and hence, on the amount of actin recruited. This data
433 is consistent with actin supplying the forces necessary for membrane scission. The membrane
434 invagination continues until the “right” amount of actin is recruited. At this amount of actin, enough
435 forces are generated to rupture the membrane. The amount of force necessary is determined by
436 the physical properties of the membrane like membrane rigidity, tension, and proteins accumulated
437 on the membrane (Dmitrieff and Nedelec, 2015). Vesicle scission releases membrane-bound Rvs,
438 resulting in release of the SH3 along with BAR domains. Release of the SH3 domains could indicate
439 to its binding partner in the actin network that vesicle scission has occurred, beginning disassembly
440 of actin components. In BAR strains, a low amount of actin is recruited (Fig.3.4C). Although the
441 absence of the SH3 domain severely perturbs the actin network, the mechanistic effect of this
442 perturbation is unclear.

443 **Model for membrane scission**

444 I propose that Rvs is recruited to sites by two distinct mechanisms. SH3 domains cluster Rvs
445 at endocytic sites. This SH3 interaction increases the efficiency with which the BAR domains
446 sense curvature on tubular membranes. BAR domains bind to endocytic sites by sensing tubular
447 membrane. BAR domains are recruited over the entire membrane tube, but do not form a tight
448 helical scaffold. Membrane shape is stabilized against fluctuations that could cause scission by
449 the BAR-membrane interaction. This prevent actin forces from rupturing the membrane, and the
450 invaginations continue to grow in length as actin continues to polymerize. BAR recruitment to
451 membrane tubes is restricted by the surface area of the tube: after a certain amount of Rvs, the
452 excess interacts with endocytic sites via the SH3 domain. Adding over a certain amount of Rvs also
453 does not increase the stabilization effect on the tube. As actin continues to polymerize, at a certain
454 amount of actin, enough forces are generated to overcome the resistance to membrane scission
455 provided by the BAR scaffold. The membrane ruptures, and vesicles are formed. Synaptojanins
456 may help recruit Rvs at endocytic sites: Inp51 and Inp52 have proline rich regions that could act as
457 binding sites for Rvs167 SH3 domains. They are involved in vesicle uncoating post-scission, likely by
458 dephosphorylating PIP2 and inducing disassembly of PIP2-binding endocytic proteins. Eventually
459 phosphorylation regulation allows endocytic proteins to be reused at endocytic sites, while the
460 vesicle is transported elsewhere into the cell.

461 Morbi luctus, wisi viverra faucibus pretium, nibh est placerat odio, nec commodo wisi enim eget
462 quam. Quisque libero justo, consectetur a, feugiat vitae, porttitor eu, libero. Suspendisse sed
463 mauris vitae elit sollicitudin malesuada. Maecenas ultricies eros sit amet ante. Ut venenatis velit.
464 Maecenas sed mi eget dui varius euismod. Phasellus aliquet volutpat odio. Vestibulum ante ipsum
465 primis in faucibus orci luctus et ultrices posuere cubilia Curae; Pellentesque sit amet pede ac sem
466 eleifend consectetur. Nullam elementum, urna vel imperdiet sodales, elit ipsum pharetra ligula,
467 ac pretium ante justo a nulla. Curabitur tristique arcu eu metus. Vestibulum lectus. Proin mauris.

468 Proin eu nunc eu urna hendrerit faucibus. Aliquam auctor, pede consequat laoreet varius, eros
469 tellus scelerisque quam, pellentesque hendrerit ipsum dolor sed augue. Nulla nec lacus.

470 Methods and Materials

471 Guidelines can be included for standard research article sections, such as this one.

472 Nulla malesuada porttitor diam. Donec felis erat, congue non, volutpat at, tincidunt tristique,
473 libero. Vivamus viverra fermentum felis. Donec nonummy pellentesque ante. Phasellus adipiscing
474 semper elit. Proin fermentum massa ac quam. Sed diam turpis, molestie vitae, placerat a, molestie
475 nec, leo. Maecenas lacinia. Nam ipsum ligula, eleifend at, accumsan nec, suscipit a, ipsum.
476 Morbi blandit ligula feugiat magna. Nunc eleifend consequat lorem. Sed lacinia nulla vitae enim.
477 Pellentesque tincidunt purus vel magna. Integer non enim. Praesent euismod nunc eu purus.
478 Donec bibendum quam in tellus. Nullam cursus pulvinar lectus. Donec et mi. Nam vulputate metus
479 eu enim. Vestibulum pellentesque felis eu massa.

480 Citations

481 LaTeX formats citations and references automatically using the bibliography records in your .bib
482 file, which you can edit via the project menu. Use the \cite command for an inline citation, like
483 ?, and the \citet command for a citation in parentheses (?). The LaTeX template uses a slightly-
484 modified Vancouver bibliography style. If your manuscript is accepted, the eLife production team
485 will re-format the references into the final published form. *It is not necessary to attempt to format*
486 *the reference list yourself to mirror the final published form.* Please also remember to **delete the line**
487 **\nocite{*}** in the template just before \bibliography{...}; otherwise *all* entries from your .bib
488 file will be listed!

489 Acknowledgments

490 Additional information can be given in the template, such as to not include funder information in
491 the acknowledgments section.